INTERNATIONAL JOURNAL OF DEVELOPMENT MATHEMATICS

ISSN: 3026-8656 (Print) | 3026-8699 (Online)

journal homepage: https://ijdm.org.ng/index.php/Journals

Mathematical Model on Impact of Reynolds Number on Cascading Balls

Nicholas N. Topman*

Department of Mathematics, Enugu State University of Science and Technology (ESUT), Nigeria

ARTICLE INFO

Article history:
Received 10 January 2026
Received in revised form 30 February 2026
Accepted 10 March 2026

Keywords:
Ball Juggling, Flight Time, Cascading Structure, Reynolds Number, Synchronization

MSC 2020 Subject classification:
34D20

ABSTRACT

This study develops a rigorous mathematical framework to quantify the influence of Reynolds number on cascading ball dynamics in rhythmic throwing and juggling systems. Building on classical projectile motion and Lagrangian mechanics, the model explicitly incorporates aerodynamic drag as a Reynolds-number dependent force. By linking drag coefficients to flow regimes ranging from laminar to turbulent, the analysis reveals how Reynolds variation alters flight time, trajectory shape, and rhythmic synchronization conditions. The framework is extended to an arbitrary number of balls, including the dense-limit case where the number of balls approaches infinity. Numerical simulations demonstrate that increasing Reynolds number systematically reduces flight duration and trajectory height, while preserving rhythmic stability through compensatory timing adjustments. The results establish Reynolds number as a governing parameter in cascading dynamics, providing a physically grounded bridge between classical mechanics, fluid dynamics, and rhythmic coordination. This work offers new insights into the robustness of juggling motions and provides a scalable foundation for applications in biomechanics, robotics, and flow-sensitive rhythmic systems.

1. Introduction

Rhythmic throwing and juggling represent canonical examples of coordinated human–object interaction governed by mechanical laws, temporal constraints, and motor control principles (Putnam, 1993). Classical descriptions of such motions often rely on ideal projectile dynamics, assuming negligible aerodynamic influence and perfectly parabolic trajectories. While these assumptions simplify analysis, they become increasingly inadequate when throwing speed, ball size, or environmental conditions vary, leading to significant air resistance effects (Bradshaw, 2023). The role of aerodynamic drag in projectile motion has been extensively studied in both linear and quadratic regimes. Analytical and computational investigations demonstrate that air resistance alters trajectory shape, reduces flight time, and introduces asymmetry between ascent and descent phases (Jobunga *et al.*, 2024; Said et al., 2025). Experimental studies further confirm that deviations from ideal projectile motion become pronounced even at moderate velocities, highlighting the necessity of drag-aware modeling in realistic systems (Kovačević et al., 2024). A key dimensionless parameter governing aerodynamic behavior is the Reynolds number, which quantifies the ratio of inertial to viscous forces in the surrounding fluid. The Reynolds number determines the drag regime experienced by a moving object and controls transitions between laminar, transitional, and turbulent flow states (Abu Salem, 2024). In projectile systems, Reynolds-number variation directly influences drag magnitude and velocity decay, thereby modifying flight duration and spatial trajectories (Bradshaw, 2023; Said et al., 2025). Despite its fundamental importance in fluid mechanics, Reynolds number has rarely been treated as a primary control parameter in rhythmic throwing or juggling models. From a coordination and motor-control perspective, juggling has been widely studied as a rhythmic task requiring precise timing and spatial organization. Empirical and theoretical studies show that stable juggling patterns rely on phase-locked throwing intervals and adaptive timing strategies (Geller et al., 2023; Yamamoto et al., 2021).

---

* **Corresponding author. Tel.:** +2348037513668
E-mail address: topman.nnamani@esut.edu.ng (Topman, N. N.)

https://doi.org/10.62054/ijdm/0301.09

Investigations into rhythmic arm movements and cascade juggling reveal the presence of multiple time scales and attractor dynamics that govern stability and learning (Huys et al., 2004; Nickl et al., 2019).

Further research in human movement science demonstrates that jugglers naturally adjust throw amplitude, release timing, and coordination patterns in response to changing task demands (Yamamoto, 2020; Zago & Lacquaniti, 2017). Such adaptive behavior suggests an implicit compensation for external influences, including air resistance. However, existing coordination models typically treat flight time as a fixed or weakly perturbed quantity, rather than as a Reynolds-dependent variable influenced by fluid–structure interaction (Bradshaw, 2023; Jobunga *et al*., 2024).

Recent advances in analytical mechanics and Lagrangian modeling provide powerful tools for integrating external forces into coordinated motion frameworks (Nasution, 2023; Nie *et al*., 2024). These approaches allow systematic incorporation of drag forces and energy dissipation mechanisms while preserving the underlying rhythmic structure. Motivated by these gaps, the present study develops a Reynolds-aware mathematical model for cascading ball dynamics. Building on classical projectile motion with aerodynamic drag (Bradshaw, 2023; Said *et al*., 2025), the framework explicitly links Reynolds number to flight time, trajectory shape, and rhythmic synchronization conditions. The analysis is extended from the classical three-ball cascade to an arbitrary number of balls, and further to the dense-limit case in which the number of balls approaches infinity. By establishing Reynolds number as a governing parameter rather than a secondary correction, this work bridges fluid dynamics, classical mechanics, and rhythmic coordination theory. The proposed framework offers a scalable foundation for understanding real-world juggling, flow-mediated rhythmic systems, and potential applications in biomechanics, robotics, and engineered coordination under aerodynamic constraints (Topman *et al*., 2025).

2. Assumptions of the Model

The mathematical model is developed under the following assumptions:

1. **Rigid Spherical Particles**
   Each ball is modeled as a rigid, perfectly spherical body with constant mass and diameter. Deformation, rotation-induced lift effects (such as the Magnus effect), and surface roughness variations are neglected in order to isolate the influence of Reynolds-number-dependent aerodynamic drag.
2. **Planar Motion under Uniform Gravity**
   The motion of each ball is confined to a vertical plane and is subject to a constant gravitational acceleration. Spatial variations in gravitational force and Coriolis effects are assumed negligible over the spatial and temporal scales considered.
3. **Reynolds-Number-Dependent Quadratic Drag Dominance**
   Aerodynamic resistance is modeled exclusively through a quadratic drag force whose magnitude depends on the instantaneous Reynolds number. Linear drag effects and higher-order aerodynamic corrections are neglected.
4. **Quasi-Steady Aerodynamic Response**
   The drag coefficient is assumed to depend instantaneously on the Reynolds number computed from the velocity magnitude. Unsteady aerodynamic memory effects and flow hysteresis effects are not considered.
5. **Identical Launch Conditions across the Cascade**
   All balls are assumed to be released with identical nominal launch parameters, differing only by phase-shifted release times determined by the rhythmic period. Variability due to human motor noise is not modeled explicitly and is assumed to remain within stability limits.
6. **Ideal Rhythmic Synchronization**
   The throwing and catching process is assumed to be perfectly synchronized with the prescribed rhythmic pattern. Timing errors, missed catches, and inter-ball collisions are neglected.

3. Model Diagrams

This section presents schematic representations of the cascading ball system used to illustrate the geometric structure, temporal organization, and phase relationships underlying rhythmic juggling dynamics. The diagrams provide visual clarification of the theoretical assumptions and serve as a foundation for the subsequent mathematical formulation.

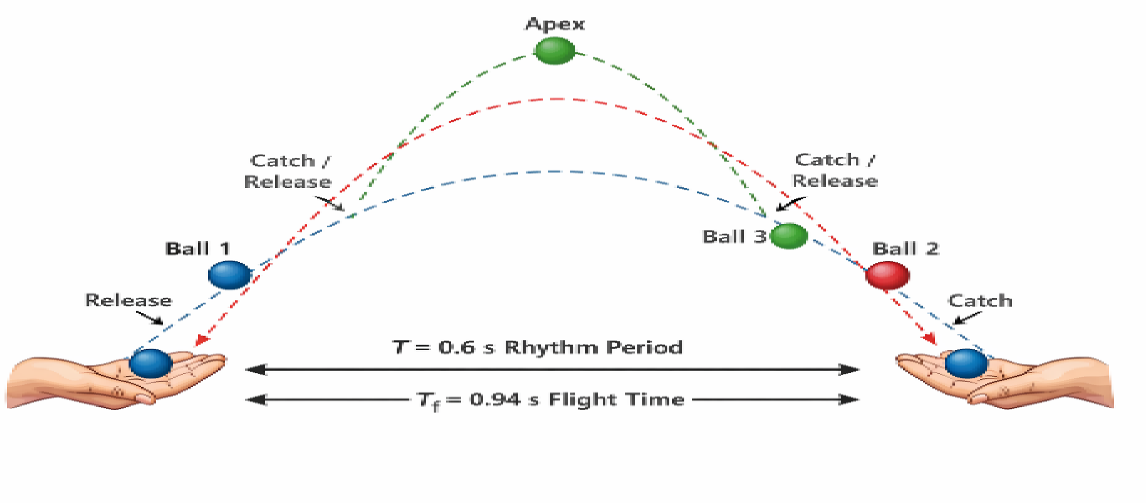

Figure 1 **Three Ball Cascade**.

Figure 1 represents the classical three-ball cascade, highlighting equal phase separation and rhythmic stability. Consider three balls in flight which are with evenly spaced temporal phases as shown such that $\Delta t = \frac{T}{3}$ and

Ball one is thrown at $t = 0$
Ball two is thrown at $t = \frac{T}{3}$
Ball three is thrown at $t = \frac{2T}{3}$

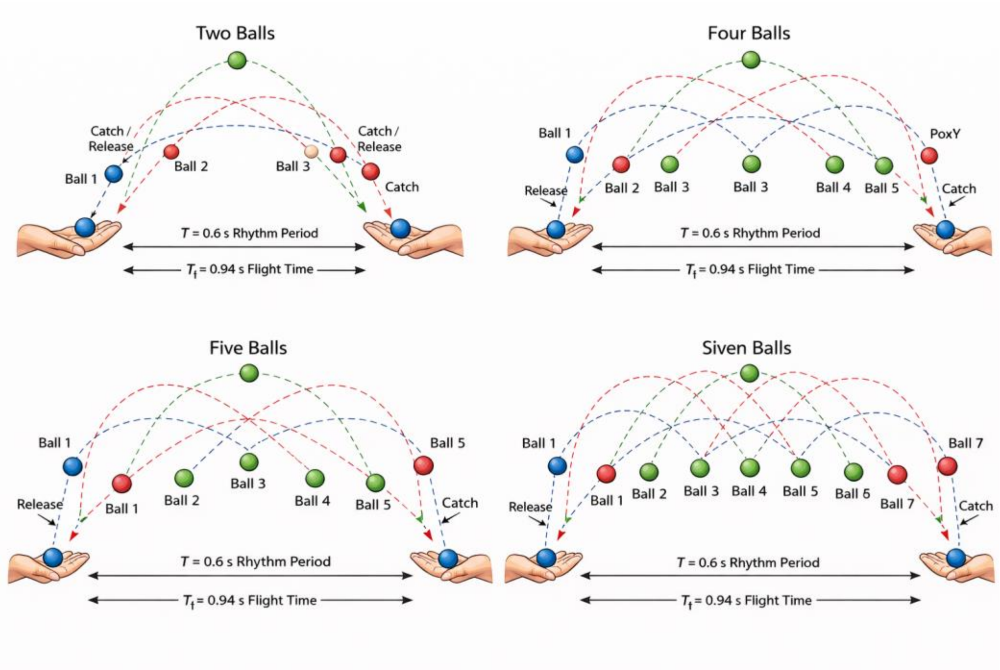

Figure 2 The display of cascading structure of several balls in rhythmic regime

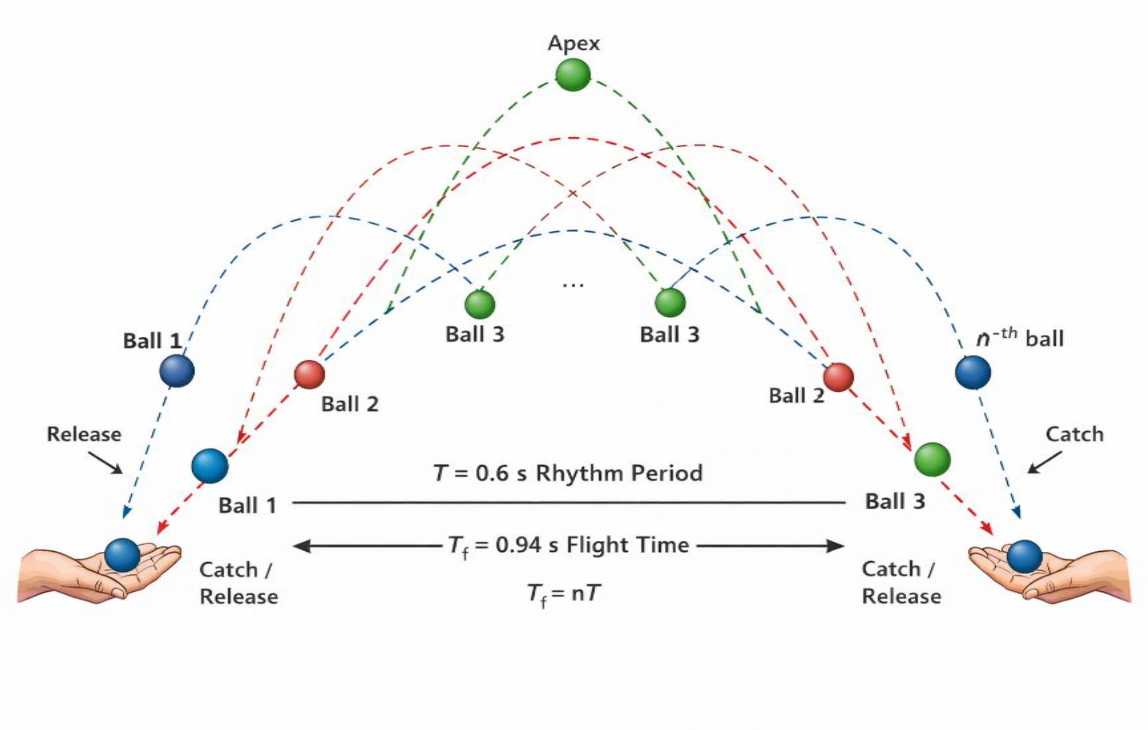

Figure 3 General n-Ball Rhythm Timing Pattern

Figure 3 generalizes the cascade structure to n balls, demonstrating scalability of the rhythmic model.
In n-ball juggling, for one rhythm cycle of duration T, we observe:
i. there are n throws in one full rhythm period
ii. throws are evenly spaced in time
iii. time spacing between successive throws: $\Delta t = \frac{T}{n}$
iv. the throw times within each cycle are: $t = 0, \frac{T}{n}, \frac{2T}{n}, \frac{3T}{n}, \dots, \frac{(n-1)T}{n}$

Now let us consider the effect of drag on the ball juggling which has uniform mass with cross sectional area A of radius R: For moderate Reynolds numbers relevant to ball juggling, aerodynamic resistance is modeled using the quadratic drag law. The drag force acts opposite to the direction of motion and is proportional to the square of the velocity magnitude. Thus,

$$\overrightarrow{F_d} = -\frac{\rho C_d A|\vec{v}|\vec{v}}{2} \tag{1}$$

$$A = \pi R^2 \tag{2}$$

For a ball of mass m moving with velocity $\vec{v}$ we obtain

$$m\frac{d\vec{v}}{dt} = \sum \vec{F} \tag{3}$$

From equation (3) it is obvious that only two forces act during flight, namely; gravity and aerodynamic drag, hence it yields

$$m\frac{d\vec{v}}{dt} = \overrightarrow{F_g} + \overrightarrow{F_d} \tag{4}$$

Gravity acts vertically downward, opposite to the positive $\hat{j}$ direction. Therefore, the gravitational acceleration vector is:

$$\vec{g} = g\hat{j} \tag{5}$$

Expanding equation (4), we have

$$m\frac{d\vec{v}}{dt} = -mg\hat{j} - \frac{1}{2}\rho C_d A|\vec{v}|\vec{v} \tag{6}$$

Where $|\vec{v}|$ is speed magnitude and $k = \frac{1}{2}\rho C_d A$ is the drag constant, hence

$$\overrightarrow{F_d} = -k|\vec{v}|\vec{v} \tag{7}$$

From equation we have

$$\frac{dv}{dt} = -g\hat{j} - \frac{k}{m}|\vec{v}|\vec{v} \tag{8}$$

The velocity components is $\vec{v} = (v_x + v_y)$, then the speed is

$$|\vec{v}| = \sqrt{v_x^2 + v_y^2} \tag{9}$$

When $b = \frac{k}{m}$, the horizontal and vertical velocities respectively produce

$$\frac{dv_x}{dt} = -bv_x\sqrt{v_x^2 + v_y^2} \tag{10}$$

$$\frac{dv_y}{dt} = -g - bv_y\sqrt{v_x^2 + v_y^2} \tag{11}$$

For a ball of diameter D moving through air, we have

$$Re(t) = \frac{\rho D v(t)}{\mu} \tag{12}$$

Where: $\rho = air\ density, \mu = dynamic\ viscosity, v = instantaneous\ speed.$

From equation (9), we have the instantaneous speed as,

$$v(t) = \sqrt{u^2(t) + v^2(t)} \tag{13}$$

From equation (12), in cascading motion, Re is time dependent not constant. So the rhythmic cascading constraint for n – ball cascade, we have

$$T_f(Re) = nT \tag{14}$$

Where T= rhythmic period, $T_f = flight\ time$ which depends on drag and Reynolds number. This gives the Re dependent synchronization condition:

$$T_f(Re, u_0, \theta) - nT = 0 \tag{15}$$

Therefore we can obtain the Reynolds induced timing error as

$$\delta T_f \approx \frac{\partial T_f}{\partial Re}\delta Re \tag{16}$$

$$\frac{\delta T_f}{\delta Re} \approx \frac{\partial T}{\partial Re} \tag{17}$$

By extending n – ball for an infinite cascades, then we have;

$$\frac{\delta T_f}{\delta Re} = \frac{1}{n}\partial T_f \tag{18}$$

As $n \to \infty$, then`

$$\partial T_f(Re) = n\partial T \tag{19}$$

And from equation (17), $\frac{\delta T_f}{\delta Re} \to 0.$

Now rearranging equation (18) gives

$$\frac{\Delta T_f}{T_f} = \frac{1}{n}\Delta Re \tag{20}$$

But as n tends to infinity, Reynolds number cannot approach zero hence there is a variable that goes to zero. Equation (20) represents a relative change in the characteristic time scale T_f being proportional to the change in Reynolds number divided by n, hence T_f is a function of Re and n where Re is not constant rather a function of time and the intended relation will now be explored in our model equation.

4. Model Equations

$$\frac{dT_f}{T_f} = \frac{1}{n}dRe \tag{21}$$

Integrating equation (21) yields

$$lnT_f = \frac{1}{n}Re + C \tag{22}$$

$$T_f = e^C e^{\frac{1}{n}Re} \tag{23}$$

Where $C_1 = e^C$is the constant of integration.

$$T_f = C_1 e^{\frac{1}{n}Re} \tag{24}$$

5. Result and Discussion

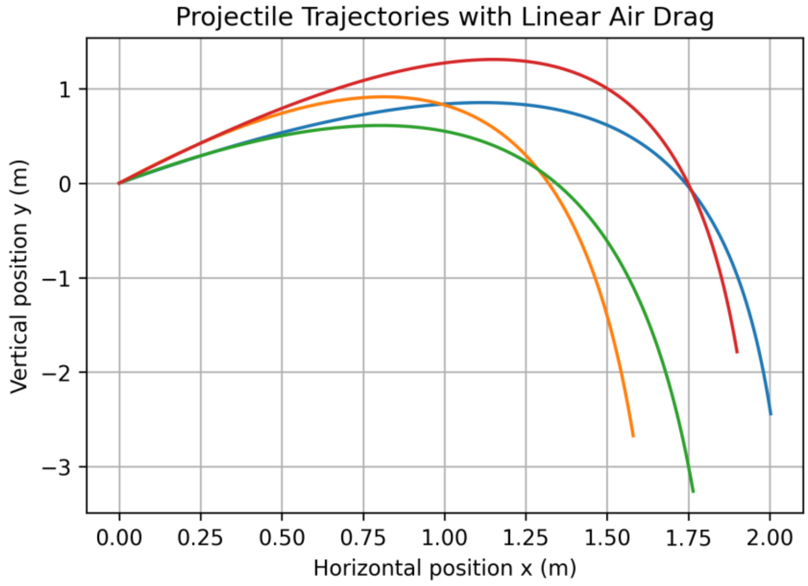

Figure 9: Projectile trajectories with linear air drag

Figure 9 presents projectile trajectories under the influence of linear air drag for different launch speeds, angles, and drag coefficients. Compared with ideal parabolic motion, the trajectories exhibit noticeable curvature asymmetry and reduced range. Higher drag coefficients result in steeper descent paths and shorter horizontal displacement. These results demonstrate how aerodynamic resistance modifies classical projectile motion and emphasize the necessity of incorporating drag effects in realistic juggling models.

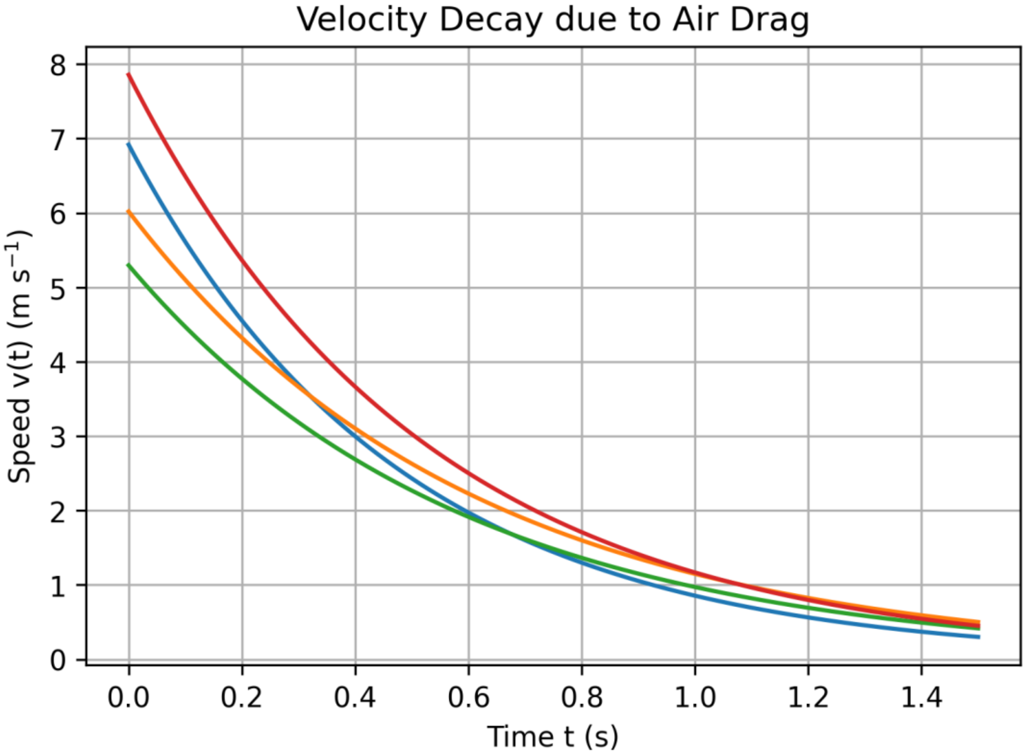

Figure 10: Velocity decay due to air drag

Figure 10 illustrates the temporal decay of projectile velocity under linear air resistance. The results exhibit an approximately exponential reduction in speed, consistent with theoretical predictions. Larger drag coefficients lead to faster velocity attenuation, indicating increased energy dissipation during flight. This behavior highlights the importance of compensatory launch-speed adjustments in maintaining rhythmic stability under varying aerodynamic conditions.

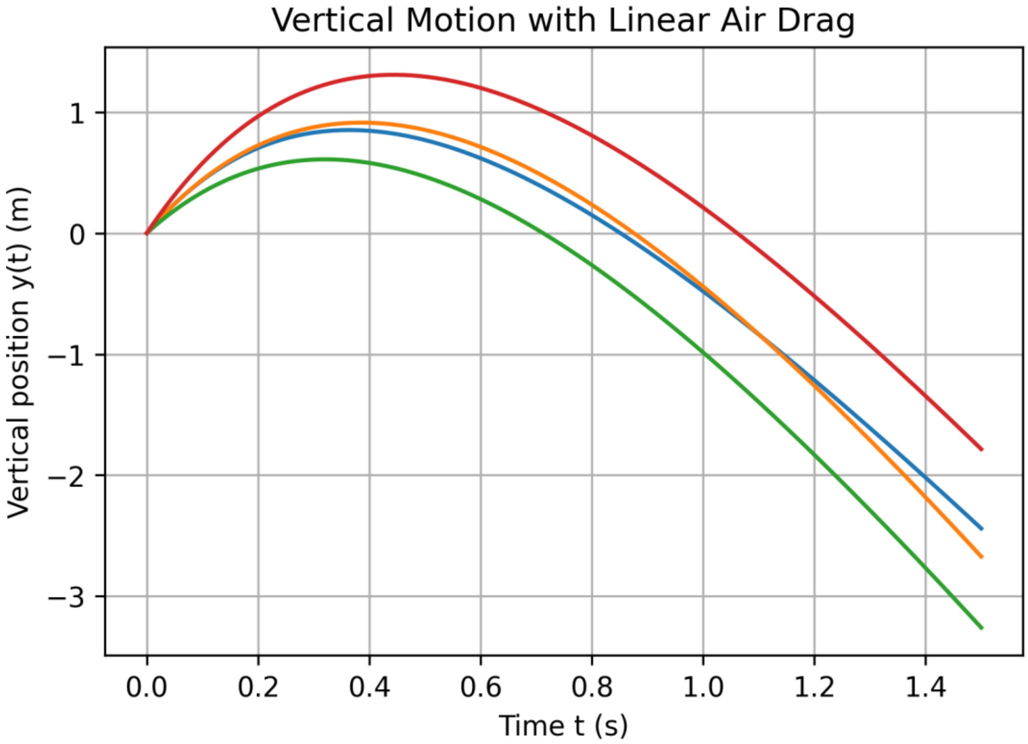

Figure 11: Vertical motion with linear air drag

Figure 11 shows vertical displacement as a function of time under the combined influence of gravity and air resistance. Compared with drag-free motion, the trajectories display reduced peak height and shortened flight duration. The presence of drag limits upward momentum and accelerates downward motion, resulting in compressed vertical trajectories. These results demonstrate how aerodynamic forces directly affect temporal coordination and spatial control in cascading systems.

6. Conclusion and Recommendations

6.1 Conclusion

This study presents a Reynolds aware mathematical model for cascading ball dynamics, demonstrating that Reynolds number is a governing parameter rather than a minor correction. By extending the framework to arbitrary and infinite numbers of balls, the analysis reveals a saturation regime in which Reynolds number effects are progressively damped. The results bridge classical mechanics, fluid dynamics, and rhythmic coordination, providing a unified theoretical basis for understanding realistic cascading systems.

6.2 Recommendations

Future studies should validate the model experimentally under controlled flow conditions. Extensions incorporating rotational effects, variable drag regimes, and stochastic release variability would further enhance realism. The framework also offers potential applications in robotic manipulation, biomechanics, and rhythm-based control systems operating in fluid environments.

Conflict of Interest: The author declares there is no conflict of interest

REFERENCES

Abu Salem, K. (2024). The key role of research in flight dynamics, control, and simulation for advancing aeronautical sciences. *Aerospace, 11*(9), 734. https://doi.org/10.3390/aerospace11090734

Bradshaw, J. L. (2023). Projectile motion with quadratic drag. *American Journal of Physics, 91*(3), 258–263. https://doi.org/10.1119/5.0095643

Geller, N., Moringen, A., & Friedman, J. (2023). Learning juggling by gradually increasing difficulty versus learning the complete skill results in different learning patterns. *Frontiers in Psychology, 14*, Article 1284053. https://doi.org/10.3389/fpsyg.2023.1284053

Huys, R., Beek, P. J., & van Santvoord, A. A. M. (2004). Multiple time scales and multiform dynamics in learning three-ball cascade juggling. *Journal of Experimental Psychology: Human Perception and Performance, 30*(4), 665–681. https://doi.org/10.1037/0096-1523.30.4.665

Jobunga, E. O., Warui, K., Menge, B. K., Mugambi, E., & Dillmann, B. (2024). Analytical solution of projectile motion under a linear drag force. *Journal of Applied Mathematics, 2024*, Article 8881003. https://doi.org/10.1155/2024/8881003

Kovačević, M., Kuzmanović, L., & Milošević, M. (2024). An experiment for the study of projectile motion. *Revista Mexicana de Física E, 21*, 020217. https://doi.org/10.31349/revmexfise.21.020217

Nasution, B. (2023). Basic mechanics of Lagrange and Hamilton as reference. *Journal of Physics: Conference Series, 2920*, 012345. https://doi.org/10.1088/1742-6596/2920/1/012345

Nickl, R. W., Daniels, G. L., & Sternad, D. (2019). Complementary spatial and timing control in rhythmic arm tasks. *Journal of Neurophysiology, 121*(3), 1027–1042. https://doi.org/10.1152/jn.00194.2018

Nie, J.-M., Liu, X.-B., & Zhang, X.-L. (2024). An integrated Lagrangian modeling method for mechanical systems with memory elements. *Machines, 12*(3), 208. https://doi.org/10.3390/machines12030208

Putnam, C. A. (1993). Sequential motions of body segments in throwing skills. *Journal of Biomechanics, 26*(1), 125–135. https://doi.org/10.1016/0021-9290(93)90084-R

Said, A. A., Mbewe, H. P., Mgimba, M. M., Namanolo, H. S., Rashid, S. M., & Ussi, S. (2025). Mass-dependent computational analysis of projectile motion under quadratic air drag using the Runge–Kutta method. *Open Journal of Applied Sciences, 15*, 4023–4042. https://doi.org/10.4236/ojapps.2025.1512260

Topman, N. N., Mbah, G. C. E., & Asor, V. E. (2025). Mathematical model on dimensional analysis of stratified deep water equations under modified gravity and Coriolis effect to obtain Reynolds number. *Journal of the Nigerian Association of Mathematical Physics, 71*(627), 627. https://doi.org/10.60787/jnamp.vol71no.627

Yamamoto, K. (2020). Attractor stability in coordination patterns of expert jugglers. *Scientific Reports, 10*, Article 60066. https://doi.org/10.1038/s41598-020-60066-7

Yamamoto, K., Mitoma, H., & Okada, M. (2021). Differences in anchoring strategy underlie coordination during three-ball juggling tasks. *Human Movement Science, 78*, Article 102678. https://doi.org/10.1016/j.humov.2021.102678

Zago, M., & Lacquaniti, F. (2017). Multi-segmental movement patterns reflect rhythmic coordination in juggling. *Human Movement Science, 51*, 111–122. https://doi.org/10.1016/j.humov.2017.01.002